PCCP

How well do self-interaction corrections repair the over-estimation of molecular polarizabilities in density functional calculations?

Journal:	*Physical Chemistry Chemical Physics*
Manuscript ID	CP-ART-12-2020-006512.R4
Article Type:	Paper
Date Submitted by the Author:	19-Jul-2021

Complete List of Authors:	Akter, Sharmin ; University of Texas at El Paso, Physics Vargas Tellez, Jorge; University of Texas at El Paso, Physics; Universidad Autonoma de Zacatecas, Física Sharkas, Kamal; Central Michigan University, Department of Physics Peralta, Juan; Central Michigan University, Physics Jackson, Koblar; Central Michigan University, Physics Baruah, Tunna; University of Texas at El Paso, Physics Zope, Rajendra; University of Texas at El Paso, Physics

PCCP

ARTICLE TYPE

Cite this: DOI: 00.0000/xxxxxxxxxx

How well do self-interaction corrections repair the overestimation of static polarizabilities in density functional calculations?

Sharmin Akter,[a] Jorge A. Vargas,[b] Kamal Sharkas,[c] Juan E. Peralta,[c] Koblar A. Jackson,[c*] Tunna Baruah,[ad] and Rajendra R. Zope[ad*]

Received Date
Accepted Date

DOI: 00.0000/xxxxxxxxxx

We examine the effect of removing self-interaction error (SIE) on the calculation of molecular polarizabilities in the local spin density (LSDA) and generalized gradient approximations (GGA). To this end, we utilize a database of 132 molecules taken from a recent benchmark study [*Hait and Head-Gordon, Phys. Chem. Chem. Phys. 2018,* ***20****, 19800*] to assess the influence of SIE on polarizabilities by comparing results with accurate reference data. Our results confirm that the general overestimation of molecular polarizabilities by these density functional approximations can be attributed to SIE. However, removing SIE using the Perdew-Zunger self-interaction-correction (PZ-SIC) method, implemented using the Fermi-Löwdin Orbital SIC approach, leads to an underestimation of molecular polarizabilities, showing that PZ-SIC overcorrects when combined with LSDA or GGA. Application of a recently proposed locally scaled SIC [*Zope et al., J. Chem. Phys. 2019,* ***151****, 214108*] is found to provide more accurate polarizabilities. We attribute this to the ability of the local scaling scheme to selectively correct for SIE in the regions of space where the correction is needed most.

1 Introduction

Correctly modeling the behavior of molecular complexes requires an electronic structure method that accurately describes the interaction of a molecule with an external electric field. This is necessary, for example, to properly describe the response[1,2] of a molecule to the dipole of a second, neighboring molecule. The static dipole polarizability is therefore a key quantity, since it describes the response of a molecule's electron charge distribution to an applied field[1,3]. Post-Hartree-Fock wave function approaches, such as the coupled cluster method with singles, doubles and perturbative triples, CCSD(T)[4], successfully predict polarizabilities close to experimental values for systems with predominantly single–reference character,[5] but can be computationally expensive for large molecules. Kohn-Sham density functional theory (DFT)[6–8] is a computationally efficient alternative, but the accuracy of DFT calculations depends on the density functional approximation (DFA) used. A number of studies have been carried out to assess the performance of DFAs for predicting polarizabilities.[9–17] Recently, Hait and Head-Gordon[5] compared the results of 60 DFAs for the static polarizabilities of 132 atoms and small molecules to CCSD(T) reference values. The results show that the calculated polarizabilities generally improve with the sophistication of the DFAs, from local spin density approximations (LSDAs), to generalized gradient approximations (GGAs), to meta-GGAs, but with a general tendency to overestimate reference values. Self-interaction error (SIE) is identified in Ref. 5 as the likely explanation for the overestimation by the DFAs, justified because partially removing SIE via the use of hybrid DFAs improves the results. SIE originates from an incomplete cancellation of the self-Coulomb energy by the self-exchange energy in a DFA, causing the effective potential seen by an electron in a DFA calculation to decay exponentially, instead of as $-1/r$, for a neutral finite system. This, in turn, results in valence electrons that are too weakly bound and polarizabilities that are too large.

The Perdew–Zunger self–interaction correction (PZ–SIC)[18] removes the SIE from a DFA on an orbital-by-orbital basis, and it has been used in numerous studies of the effects of SIE in calculations for atoms, molecules, and solids.[19–71] The failure of

[a]*Computational Science Program, The University of Texas at El Paso, El Paso, Texas, 79968*
[b] *Unidad Academica de Física, Universidad Autónoma de Zacatecas, Calz. Solidaridad Esq. Paseo de la Bufa S N, Zacatecas, México. C.P. 98060*
[c]*Physics Department and Science of Advanced Materials Program, Central Michigan University, Mt. Pleasant Michigan, 48859*
[d]*Department of Physics, The University of Texas at El Paso, El Paso, Texas, 79968*
[*]*email: jacks1ka@cmich.edu*
[†]*email: rzope@utep.edu*
† Electronic Supplementary Information (ESI) available: [details of any supplementary information available should be included here]. See DOI: 10.1039/cXCP00000x/

density functional approximations (DFAs) in the prediction of dipole and higher-order polarizabilities, especially, for molecular chains and polymers has been discussed extensively by several groups.[50,64,72–90]

Recent calculations showed that the use of PZ-SIC led to improved polarizabilities for atoms from H to Ar[88] and for water clusters from monomer to hexamers[89]. Removing SIE tended to decrease the DFA polarizabilities toward accurate reference values, but in a majority of cases resulted in over-correction, yielding polarizabilities that are too small. A similar over-correction has been found for properties such as bond lengths and atomization energies, prompting attempts to scale down the magnitude of the SIC terms in PZ-SIC.[47,48,91] Santra and Perdew recently provided insight into the over-correction problem, demonstrating that removing self-interaction from standard DFAs using the PZ approach results in incorrect exchange-correlation energies in the limit of uniform densities where the DFAs are correct by construction[92]. Zope *et al.*[93] recently proposed a locally scaled self-interaction correction (LSIC), where the SIC energy density is scaled at each point in space depending on the nature of the density at that point. The scaling parameter was chosen to eliminate the SIC for uniform densities, while applying full SIC when the density is one-electron-like. The result is a method that, like PZ-SIC, is exact for any one-electron density, but unlike PZ-SIC, is also exact for uniform densities. LSIC, when combined with the PW92 LSDA functional[94] (LSIC-LSDA), provides[93] results that are comparable to PZ-SIC-LSDA for properties like chemical reaction barriers that are strongly impacted by SIE, while also yielding significantly better atomization energies than those of LSDA and PZ-SIC-LSDA, with results comparable to, or better than, those obtained using the Perdew, Burke, and Ernzerhof (PBE) GGA[95].

The purpose of the present work is to assess how removing SIE affects the performance of DFAs in predicting the static dipole polarizabilities of molecules using both PZ-SIC and LSIC. To this end, we employ an implementation of both approaches within the Fermi-Löwdin orbital (FLO)-SIC framework,[96,97] and we evaluate the static dipole polarizabilities of the atoms and molecules in the benchmark set of Hait and Head-Gordon[5] using LSDA and PBE and their PZ-SIC and LSIC counterparts, and compare the results with the CCSD(T) values of Ref. 5.

2 Methods and computational details

In PZ-SIC, the exchange-correlation (XC) energy is given by

$$E_{\rm XC}^{\rm SIC-DFA}[\rho_\uparrow,\rho_\downarrow] = E_{\rm XC}^{\rm DFA}[\rho_\uparrow,\rho_\downarrow] - \sum_{i,\sigma}^{N_\sigma}\{U[\rho_{i\sigma}] + E_{\rm XC}^{\rm DFA}[\rho_{i\sigma},0]\}, \quad (1)$$

where i runs over the N_σ occupied orbitals of spin σ, and $\rho_{i\sigma}$ is the i^{th} orbital density. The terms $U[\rho_{i\sigma}]$ and $E_{\rm XC}^{\rm DFA}[\rho_{i\sigma},0]$ are the exact self-Coulomb and approximate self-exchange-correlation energies, respectively. $E_{\rm XC}^{\rm SIC-DFA}$ is orbital-dependent; its value depends on the choice of the orbitals used to compute it. Because of the self-Coulomb term in Eq. 1, the energy-minimizing orbitals tend to be localized. Determining these orbitals in the variational implementation of PZ-SIC requires satisfying a set of conditions known as the localization equations[98] (LE), in addition to finding the self-consistent total electron density. There are $\mathcal{O}(N^2)$ of these equations for N occupied orbitals and satisfying them is computationally expensive.

Pederson and coworkers[96] recently proposed using FLOs[99–101] as the localized orbitals in the PZ-SIC scheme. In the FLO-SIC method,[96] optimizing the FLOs replaces satisfying the LE as the means to minimize the PZ-SIC energy. The FLOs are derived from the Kohn-Sham orbitals $\psi_{j\sigma}$ as

$$\phi_{i\sigma}^{\rm FO}(\mathbf{r}) = \frac{\sum_j \psi_{j\sigma}^*(\mathbf{a}_{i\sigma})\psi_{j\sigma}(\mathbf{r})}{\sqrt{\sum_j |\psi_{j\sigma}(\mathbf{a}_{i\sigma})|^2}} = \frac{\widetilde{\rho}_\sigma(\mathbf{a}_{i\sigma},\mathbf{r})}{\sqrt{\rho_\sigma(\mathbf{a}_{i\sigma})}} \equiv \sum_j T_{ij}^\sigma \psi_{j\sigma}(\mathbf{r}), \quad (2)$$

where $\widetilde{\rho}_\sigma$ is the single-particle Kohn-Sham density matrix, and $\mathbf{a}_{i\sigma}$ are points in real space called Fermi orbital descriptors, or FODs. Any set of orbitals spanning the same occupied space leads to the same Fermi orbitals (FO), making the FLO-SIC method unitarily invariant. The FO are normalized, but not orthonormal, so they are then orthogonalized using the Löwdin symmetric orthogonalization scheme[102], yielding the orthonormal FLOs that are used to evaluate the SIC energy (Eq. 1). Since different FOD positions yield different FLOs, and therefore different total energies, minimizing the total energy in FLO-SIC implies finding optimal FOD positions. Gradients of the SIC energy with respect to the FODs can be computed[103,104], allowing the FOD positions to be optimized using standard gradient optimizers. While using the FLOs results in slightly higher total energies compared to PZ-SIC calculations in which the LE are satisfied, physical properties computed using the two approaches are virtually the same.[61]

In the LSIC method,[93] an iso-orbital indicator is used to identify the one-electron regions. In this work we use $z_\sigma(\vec{r}) = \tau_\sigma^W(\vec{r})/\tau_\sigma(\vec{r})$, where τ_σ^W and τ_σ are the von Weizsacker and total positive-definite kinetic energy densities of spin σ, respectively. This iso-orbital indicator is used to locally scale down the SIC energy density:

$$E_{\rm XC}^{\rm LSIC-DFA} = E_{\rm XC}^{\rm DFA}[\rho_\uparrow,\rho_\downarrow] - \sum_{i,\sigma}^{\rm occ}\{U^{\rm LSIC}[\rho_{i\sigma}] + E_{\rm XC}^{\rm LSIC}[\rho_{i\sigma},0]\}, \quad (3)$$

where

$$U^{\rm LSIC}[\rho_{i\sigma}] = \frac{1}{2}\int d\vec{r}\, z_\sigma(\vec{r})\,\rho_{i\sigma(\vec{r})}\int d\vec{r'}\frac{\rho_{i\sigma}(\vec{r'})}{|\vec{r}-\vec{r'}|}, \quad (4)$$

and

$$E_{\rm XC}^{\rm LSIC}[\rho_{i\sigma},0] = \int d\vec{r}\, z_\sigma(\vec{r})\,\rho_{i\sigma(\vec{r})}\,\varepsilon_{\rm XC}^{\rm DFA}[\rho_{i\sigma},0]. \quad (5)$$

z_σ is bound between 0 and 1, with 0 corresponding to the uniform electron density limit where the DFAs are exact by construction, and 1 to the one-electron density limit where the full PZ-SIC correction yields exact results. In this work, the SIC potential is scaled down using the same scaling factor, resulting in the following Hamiltonian[105],

$$H_j = -\frac{1}{2}\nabla^2 + v(\vec{r}) + \int \frac{\rho(\vec{r'})}{|\vec{r}-\vec{r'}|}d\vec{r'} + v_{\rm XC}^{\rm DFA}([\rho]) - z_\sigma(\vec{r})\left(\int \frac{\rho_j(\vec{r'})}{|\vec{r}-\vec{r'}|}d\vec{r'} + v_{\rm XC}^{\rm DFA}([\rho_j])\right). \quad (6)$$

In this Hamiltonian, terms related to the variation of the energy with respect to the scaling factor are neglected. However, using the Hamiltonian in Eq. 6 self-consistently is expected to capture the most important changes to the density brought about by the scaling. Alternatively, Eq. 6 can be viewed as a model Hamiltonian analogous to other approaches designed to provide improved results for polarizabilities and related properties.[13,106–110] Self-consistent FLO-SIC densities are used as starting densities (initial guesses) for LSIC calculations using the above Hamiltonian.

The static dipole polarizability tensor α_{ij} is defined from the expansion of the total energy E in terms of an applied static electric field $\vec{F}$:

$$E(\vec{F}) = E(0) + \sum_i \frac{\partial E}{\partial F_i}F_i + \frac{1}{2}\sum_{ij}\frac{\partial^2 E}{\partial F_i \partial F_j}F_iF_j + \cdots \quad (7)$$

$$= E(0) - \sum_i \mu_i F_i - \frac{1}{2}\sum_{ij}\alpha_{ij}F_iF_j + \cdots, \quad (8)$$

where $E(0)$ is the energy at zero electric field and μ_i and F_i are the i^{th} component of the dipole moment and the applied electric field, respectively. We compute the components of the polarizability tensor using finite differences of the dipole moment obtained in the presence of different applied fields,

$$\alpha_{ij} = \left.\frac{\partial \mu_i}{\partial F_j}\right|_{F_j=0} = \lim_{F_j\to 0}\frac{\mu_i(F_j)-\mu_i(-F_j)}{2F_j}. \quad (9)$$

Electric fields were applied in the $\pm x$, $\pm y$, and $\pm z$ directions to determine the components of the polarizability tensor for each molecule. We discuss the values of the field strengths used in Sec. III below. The isotropic polarizability α_{iso} is calculated from the trace of the polarizability tensor

$$\alpha_{iso} = \frac{1}{3}\sum_i^3 \alpha_{ii} \quad (10)$$

and used for comparisons with reference values.[5]

All calculations reported in this work were carried out using the FLOSIC code,[111] based on the Gaussian-orbital-based NRLMOL code.[112–114] NRLMOL uses Cartesian Gaussian basis sets[115] that were variationally optimized for the PBE functional. To the default basis functions, we added one diffuse single Gaussian orbital of s, p, and d-type to ensure converged polarizabilities. The exponent for these additional functions was obtained from the relation $\beta(N+1) = \beta(N)^2/\beta(N-1)$, where $\beta(N)$ is the exponent of the Nth Gaussian in the basis for a given atom. Additional information about the adequacy of these basis sets is given in the next paragraph. In all calculations we employ NRLMOL's adaptive integration grid[116]. We used the PW92 LSDA functional[94] for the entire test set and the PBE functional[95] for a subset of it. Self-consistent FLO-SIC calculations were performed using the algorithm of Pederson and coworkers[97] and an SCF convergence criterion of 10^{-8} Ha. The optimal FOD configuration for each molecule was obtained by minimizing FOD gradients[104] below a tolerance of 10^{-4} Ha/Bohr. (See the next section for further discussion of the FOD optimizations.) For brevity we refer to FLO-SIC-LSDA/FLO-LSIC-LSDA calculations as SIC-LSDA/LSIC-LSDA. The optimal FODs obtained from SIC-LSDA and SIC-PBE calculations are used in subsequent LSIC-LSDA and LSIC-PBE calculations without further relaxation.

Recently, Brakestad *et al.* reported[117] a careful study of the effect of using finite basis sets to compute static polarizabilities. They computed polarizabilities for molecules in the Hait and Head-Gordon benchmark set[5] using a multi-wavelet (MW) basis that can be adjusted to achieve the basis set limit. They report linear response (LR) PBE polarizabilities for 15 of the molecules. We repeated these calculations using the NRLMOL basis[115] with an additional exponent as described above, as well as a series of standard quantum chemistry basis sets. The GAUSSIAN software package[118] was used for the LR calculations, along with Cartesian forms of all the basis sets. The root mean square relative error (RMSRE) for the NRLMOL basis polarizabilities relative to the basis set limit MW results is 0.13%. The differences between polarizabilities computed with and without self-interaction corrections discussed below are significantly larger than this. For comparison, triple-, quadruple-, and quintuple-ζ basis sets have RMSREs of 4.25%, 1.58%, and 0.66%, respectively, relative to the MW results (see the supplementary information for more details). The root mean square (RMS) absolute polarizability error with the NRLMOL basis is 0.016 Å^3, while the triple-, quadruple-, and quintuple-ζ basis sets give RMS absolute errors of 0.051 Å^3, 0.021 Å^3, and 0.007 Å^3, respectively (see the SI for more details).

3 Results and discussion

The data set of Hait and Head-Gordon[5] contains 132 chemical species (small molecules and a few isolated atoms) of main group elements up to Cl. These were divided into two groups: the non spin-polarized (NSP) set with $N = 75$, and the spin-polarized (SP) set with $N = 57$. A subset of the NSP molecules was used to test the effect on the polarizabilities of different procedures for optimizing the FODs. In one approach, the FODs optimized in zero applied field were used for all finite field calculations without further relaxation; in the second, the zero-field optimized FODs were used as starting points for independent FOD optimizations in the finite field calculations. The differences in results between the two approaches were much smaller than the differences between PZ-SIC and DFT polarizabilities (see the supplemental information for more details). We therefore used the simpler zero-field-optimized FODs for the finite field calculations. PBE polarizabilities were calculated for the molecules in the NSP subset using field strengths of 0.01, 0.005, and 0.001 a.u., respectively. Relative to the results obtained for the smallest field strength, the results for 0.01 and 0.005 a.u. gave RMS relative differences of 2.09% and 0.48%, respectively, indicating that the results for the

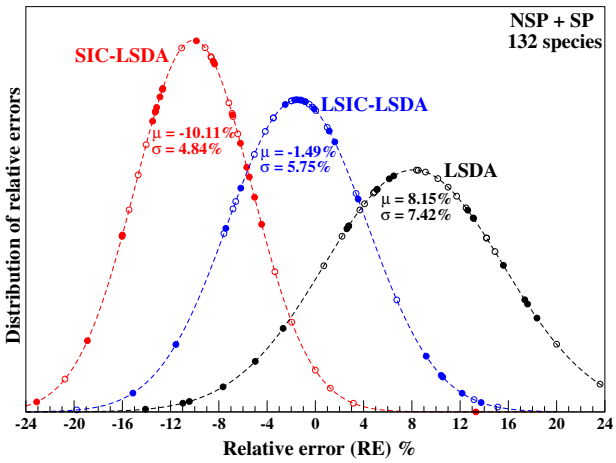

Fig. 1 Gaussian functions representing the relative errors (RE), with respect to CCSD(T), for the calculated LSDA (black), SIC–LSDA (red), and LSIC–LSDA (blue) static polarizabilities of the 132 species (NSP + SP subsets). The means (μ) and standard deviations (σ) of the Gaussians are identical to those of the respective RE distributions. The open and filled circles indicate the REs of the selected species used in Fig. 2 (NSP) and Fig. 3(SP), respectively. The choice of these "representatives" is skewed to include more examples from the tails of the distributions in order to highlight challenging cases.

smallest field are well-converged and that the 0.005 field strength gives results that are still quite accurate. For the SP subset, we followed Hait and Head-Gordon[5] and used a field strength of 0.01 a.u., except for a few of the molecules that were sensitive to the choice of field strength, for which a field strength of 0.001 was used. We tested the adequacy of the choice 0.01 a.u. for 15 of the molecules not deemed sensitive by computing PBE polarizabilities using a field strength of 0.001. The mean relative difference between the results for the two field strength choices is 1.3%.

We estimate the overall combined error in our results due to the use of a finite basis and the choice of finite field strengths to be less than 2.0%. As will be seen below, this is much smaller than the effect of self-interaction on the polarizabilities.

The statistical errors for the calculated polarizabilities, $\alpha_{\rm cal}$, compared to the CCSD(T) reference values $\alpha_{\rm ref}$,[5] are computed using the absolute, $\delta_n = \alpha_{n,\rm cal} - \alpha_{n,\rm ref}$, and relative (RE), $\varepsilon_n = ((\alpha_{n,\rm cal} - \alpha_{n,\rm ref})/\alpha_{n,\rm ref}) \times 100\%$, deviations. We define the mean error, ME $= \sum_{n=1}^{N} \delta_n/N$, mean absolute error, MAE $= \sum_{n=1}^{N} |\delta_n|/N$, maximum magnitude error, MAX $= \max\{\delta_n : 1 \le n \le N\}$, mean relative error, MRE $= \sum_{n=1}^{N} \varepsilon_n/N$, mean absolute relative error, MARE $= \sum_{n=1}^{N} |\varepsilon_n|/N$, root mean square relative error, RMSRE $= \sqrt{\sum_{n=1}^{N} \varepsilon_n^2/N}$, and the maximum magnitude relative error, MAXRE $= \max\{\varepsilon_n : 1 \le n \le N\}$.

Table 1 shows the statistical errors for polarizabilities calculated with the LSDA, SIC–LSDA, and LSIC–LSDA methods for the total NSP+SP, NSP, and SP test sets, along with the statistical errors of the PBE, SIC–PBE, and LSIC–PBE methods for the NSP test set. The individual isotropic polarizabilities for the molecules in both NSP and SP subsets are available in the supplementary information. To give a visual representation of the RE, we plot normalized Gaussian distributions with mean values and standard deviations equal to those of the RE results for LSDA, SIC-LSDA, and LSIC-LSDA, for the entire test set. The open and filled circles in Fig. 1 indicate the RE of representative molecules from the NSP (filled) and SP (open) subsets chosen for plotting in Fig. 2 and Fig. 3, respectively. The LSDA RE distribution (black curve) has a MRE of 8.15% and standard deviation of 7.42%, showing that LSDA polarizabilities generally overestimate the reference CCSD(T) values. Much of the width of this distribution results from the REs of the SP subset. (See the supplementary information for separate curves for the NSP and SP subsets.) The RMSRE for the LSDA results is 11.01%. The corresponding SIC-LSDA RE distribution (red curve) has a MRE of -10.11%, a standard deviation of 4.84%, and an RMSRE of 11.20%. The curve shows that SIC corrects the LSDA polarizabilities towards the reference values, on average, but overcorrects. There is significantly less spread in the SIC–LSDA REs than in the LSDA values. Finally, the LSIC–LSDA RE distribution (blue curve in Fig. 1) has a MRE of only -1.49%, a standard deviation of 5.75%, and an RMSRE of 5.92%. The LSIC–LSDA method clearly gives results intermediate between LSDA and SIC–LSDA on average, resulting in much better overall performance compared to reference values. The width of the LSIC-LSDA distribution is also intermediate between the widths of the other two.

The LSDA and PBE functionals give very similar results for the NSP subset of molecules. The ME, MAE, MRE, and MARE values shown in Table 1 are nearly identical for the two methods. For the self-interaction corrected results, SIC-PBE performs slightly better than SIC-LSDA, with, for example, a MRE of -7.45% compared to -9.82%. The RMSRE for SIC-PBE is 9.06%, compared to 10.79% for SIC-LSDA. PBE-based calculations were not performed for the SP subset.

As discussed elsewhere,[119] using a common local scaling factor for the self-Coulomb and self-exchange-correlation contributions to the total energy is formally justified when both are expressed in a gauge consistent way. This is the case for the LSDA, but not for PBE or for the strongly constrained and appropriately normed SCAN meta–GGA.[120] However, tests have shown that LSIC–PBE nonetheless produces good results in many cases[119]. For the molecules in the NSP set, Table 1 shows that the errors obtained using LSIC–PBE are very similar to the corresponding errors with LSIC–LSDA. In calculations[89] of polarizabilities for water clusters LSIC–PBE results were found to be in very good agreement with CCSD reference values.

Fig. 2 and Fig. 3 show the RE for 20 individual atoms or molecules taken from each of the NSP and SP subsets, respectively. In both figures, the species are ordered according to the RE in LSIC-LSDA, from most negative to most positive. The species are selected to cover the full range of REs, but those with large positive and large negative values are over-represented in the sampling. Outliers with LSIC–LSDA REs larger than +8% or less than -11% account for roughly one quarter of the cases shown in the figures, but represent less than 10% of all the cases. Approximately 80% of all the LSIC–LSDA REs are between -5 to 5%. The figures show that in nearly all cases SIC–LSDA corrects the LSDA polarizability toward the reference values, but overcorrects, resulting in little overall improvement to the MARE. The RE for the LSIC–LSDA polarizabilities typically lie between the LSDA and

Table 1 Statistical errors, in Å^3 (in % for RE–related errors), for the set of 132 species (NSP+SP) and the SP (N=57) and NSP (N=75) subsets using CCSD(T)[5] polarizabilities as reference. See text for the definition of the acronyms used for the errors. The last column indicates the molecules corresponding to MAX (MAXRE).

Sets (N)	Method	ME(MRE)	MAE(MARE)	RMSRE	MAX(MAXRE)	
NSP+SP	LSDA	0.15 (8.15)	0.40 (8.92)	11.01	-4.25 (57.46)	$Na_2(FH-OH)$
	SIC-LSDA	-0.48 (-10.11)	0.50 (10.37)	11.20	-5.13 (-28.71)	$Na_2(NaH)$
	LSIC-LSDA	0.01 (-1.49)	0.22 (3.91)	5.92	3.34 (-27.97)	Na(NaH)
NSP	LSDA	0.30(8.82)	0.30 (8.82)	10.28	1.03 (34.93)	NaCl(H)
	SIC-LSDA	-0.35 (-9.82)	0.37 (9.93)	10.79	-1.89 (-28.71)	NaH(NaH)
	LSIC-LSDA	-0.05 (-2.40)	0.19 (3.66)	5.65	3.03 (-27.97)	$Mg_2(NaH)$
	PBE	0.29(8.12)	0.29 (8.12)	9.23	1.67 (25.05)	Mg(NaCl)
	SIC-PBE	-0.23 (-7.45)	0.35 (8.22)	9.06	3.24 (-27.02)	$Mg_2(NaH)$
	LSIC-PBE	-0.03 (-1.84)	0.18 (3.45)	5.59	2.39 (-25.65)	Mg(NaH)
SP	LSDA	-0.04 (7.28)	0.54 (9.06)	11.90	-4.25 (57.46)	$Na_2(FH-OH)$
	SIC-LSDA	-0.65 (-10.49)	0.67 (10.96)	11.71	-5.13 (-24.65)	$Na_2(O_3)$
	LSIC-LSDA	0.09 (-0.29)	0.26 (4.24)	6.26	3.34 (26.22)	Na(Be)

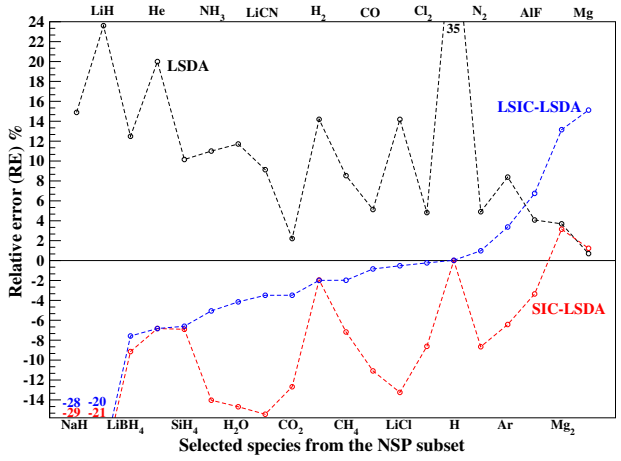

Fig. 2 The relative errors (RE), with respect to CCSD(T), for the calculated static polarizabilities of 20 species taken from the NSP subset. The REs of these 20 molecules are depicted (open circles) on the corresponding Gaussian distribution of Fig. 1. To avoid an expanded scale, some data points are replaced by the corresponding RE values.

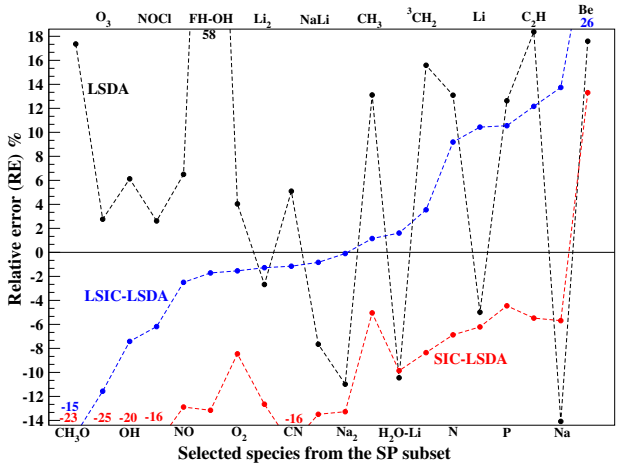

Fig. 3 The relative errors (RE), with respect to CCSD(T), for the calculated static polarizabilities of 20 species taken from the SP subset. The REs of the 20 molecules are depicted (filled circles) on the corresponding Gaussian distribution of Fig. 1. To avoid an expanded scale, some data points are replaced by the corresponding RE values.

SIC–LSDA REs. This is reasonable, given that LSIC represents a scaling down of the full SIC, but it is not always the case. In Fig. 2 there are several examples of LSIC–LSDA REs that are much closer to the SIC–LSDA values than to the LSDA values. In Fig. 3 there are many examples where the LSIC–LSDA REs are closer to the LSDA REs. In both figures there are also cases where the LSIC-LSDA REs do not fall between the LSDA and SIC–LSDA values at all.

Hait and Head-Gordon[5] used the RMSRE to rank the performance of various DFA's.[5]. For example, for the PW92 and PBE functionals, they find RMSREs of 11.93% (NSP+SP) and 9.64% (NSP only). Our corresponding results shown in Table I, 11.01% and 9.23% (NSP only), are very close to these. The SIC–LSDA and SIC–PBE RMSREs are 11.20% and 9.06%, scarcely improving over the uncorrected DFAs. On the other hand, the RMSRE for LSIC–LSDA is 5.92%, a significant improvement. This performance is better than that of the best GGA included in Ref. 5 and better than most of the meta–GGAs . The LSIC–LSDA results are competitive with those of SCAN (RMSRE = 5.31%[5]). Many of the hybrid GGA's and meta–GGAs included in Ref. 5 perform better than LSIC–LSDA, although B3LYP, perhaps the most widely-used hybrid GGA, performs[5] somewhat worse (RMSRE = 6.24%). The hybrid functionals partly address SIE by admixing a fraction of orbital-dependent Hartree-Fock-type exchange into the DFA.

Nine species were identified in Ref. 5 as the most challenging for DFAs: Be, H, CN, C_2H, H_2O-Li, Li_2, Na, NaLi, and NaH. LSIC–LSDA gives good results (errors less than 1.6% relative to the reference values) for five of these: H, CN, H_2O-Li, Li_2, and NaLi. Nevertheless, significant errors remain in the LSIC–LSDA polarizabilities for the other four molecules.

4 Summary and Conclusions

In this work we analyzed the effect of self-interaction error on molecular polarizabilities calculated using DFT methods for a database[5] of 132 molecules containing two distinct subsets, NSP($N = 75$) and SP($N = 57$). For these test sets, we evaluated

molecular polarizabilities using LSDA, SIC–LSDA, and a recently developed approach that scales down the SIC locally, LSIC–LSDA. For the NSP dataset, we also analyzed results for the PBE functional, SIC–PBE, and LSIC–PBE. We calculated various measures of the statistical errors using CCSD(T) polarizabilities[5] as the reference. Our results from both NSP and SP sets show that the plain DFAs (LSDA and PBE) significantly overestimate the polarizabilities, in line with the work of Hait and Head-Gordon.[5] The MARE is 8.92% for the complete NSP+SP data set with LSDA and 8.12% using PBE for the NSP data set. Removing self-interaction using PZ-SIC reverses this overestimation, but over corrects, giving an underestimation of the SIC–LSDA polarizabilities with a MARE of 10.37% from the CCSD(T) reference values. Use of the LSIC–LSDA method reduces the MARE to 3.91% and, while there remain cases where the RE in LSIC-LSDA polarizabilities is large, as seen in Fig. 2 and Fig. 3, LSIC–LSDA generally brings the polarizabilities for the atoms and molecules in the data set much closer to the reference CCSD(T) values. The LSIC method is designed to maintain the full PZ-SIC correction in regions in which the density is one-electron-like, while scaling down the SIC in many-electron regions, in particular in regions where the density is slowly varying. The success of LSIC–LSDA compared to SIC–LSDA suggests that PZ-SIC over-corrects for electron self-interaction in many-electron regions.

The results presented here indicate that systematic advances in the development of self-interaction free DFT methods can improve not only thermochemical, but also density-dependent properties. The point-wise scaling in the LSIC approach represents a new pathway toward accurate self-interaction free density functional approximations. The LSIC method may be further improved by identifying better iso-orbital indicators[121–123] than the ratio of kinetic energy densities used in this work, or by using the scaling functions to satisfy additional exact properties of density functionals. Research along these lines is underway.[122,123]

Data Availability Statement

The data that supports the findings of this study are available within the article and the supplementary information. See the supplementary material for additional analysis and for a listing of the calculated polarizabilities for all of the chemical species considered in this work.

Conflicts of interest

There are no conflicts to declare.

Acknowledgements

This work was supported by the US Department of Energy, Office of Science, Office of Basic Energy Sciences, as part of the Computational Chemical Sciences Program under Award No. DE-SC0018331. Support for computational time at the Texas Advanced Computing Center, the Institute for Cyber-Enabled Research at Michigan State University, and at NERSC is gratefully acknowledged.

Notes and references

1 K. D. Bonin and V. V. Kresin, *Electric-Dipole Polarizabilities of Atoms, Molecules, and Clusters*, WORLD SCIENTIFIC, 1997.
2 J. Mitroy, M. S. Safronova and C. W. Clark, *J. Phys. B: At. Mol. Opt. Phys.*, 2010, **43**, 202001.
3 A. Dalgarno, *Adv. Phys.*, 1962, **11**, 281–315.
4 J. T. Margraf, A. Perera, J. J. Lutz and R. J. Bartlett, *J. Chem. Phys.*, 2017, **147**, 184101.
5 D. Hait and M. Head-Gordon, *Phys. Chem. Chem. Phys.*, 2018, **20**, 19800–19810.
6 P. Hohenberg and W. Kohn, *Phys. Rev.*, 1964, **136**, B864–B871.
7 W. Kohn and L. J. Sham, *Phys. Rev.*, 1965, **140**, A1133–A1138.
8 R. O. Jones, *Rev. Mod. Phys.*, 2015, **87**, 897.
9 M. R. Pederson and A. A. Quong, *Phys. Rev. B*, 1992, **46**, 12906.
10 J. Guan, P. Duffy, J. T. Carter, D. P. Chong, K. C. Casida, M. E. Casida and M. Wrinn, *J. Chem. Phys.*, 1993, **98**, 4753–4765.
11 N. Matsuzawa and D. A. Dixon, *J. Chem. Phys.*, 1994, **98**, 2545–2554.
12 P. Fuentealba and Y. Simón-Manso, *J. Phys. Chem. A*, 1997, **101**, 4231–4235.
13 S. Van Gisbergen, J. Pacheco and E. Baerends, *Phys. Rev. A*, 2001, **63**, 063201.
14 P. Sałek, T. Helgaker, O. Vahtras, H. Ågren, D. Jonsson and J. Gauss, *Mol. Phys.*, 2005, **103**, 439–450.
15 R. R. Zope, T. Baruah, M. R. Pederson and B. I. Dunlap, *Int. J. Quant. Chem.*, 2008, **108**, 307–317.
16 A. J. Thakkar and T. Wu, *J. Chem. Phys.*, 2015, **143**, 144302.
17 A. L. Hickey and C. N. Rowley, *J. Phys. Chem. A*, 2014, **118**, 3678–3687.
18 J. P. Perdew and A. Zunger, *Phys. Rev. B*, 1981, **23**, 5048–5079.
19 Z. Szotek, W. Temmerman and H. Winter, *Phys. B: Condens. Matter*, 1991, **172**, 19–25.
20 J. B. Krieger, Y. Li and G. J. Iafrate, *Phys. Rev. A*, 1992, **45**, 101–126.
21 J. B. Krieger, Y. Li and G. J. Iafrate, *Phys. Rev. A*, 1992, **46**, 5453–5458.
22 E. S. Fois, J. I. Penman and P. A. Madden, *J. Chem. Phys.*, 1993, **98**, 6352–6360.
23 Y. Li, J. B. Krieger and G. J. Iafrate, *Phys. Rev. A*, 1993, **47**, 165–181.
24 T. Baruah, R. R. Zope, A. Kshirsagar and R. K. Pathak, *Phys. Rev. A*, 1994, **50**, 2191–2196.
25 M. M. Rieger and P. Vogl, 1995, **52**, 16567.
26 M. K. Harbola, *Solid State Commun.*, 1996, **98**, 629–632.
27 S. Goedecker and C. J. Umrigar, *Phys. Rev. A*, 1997, **55**, 1765–1771.
28 G. I. Csonka and B. G. Johnson, 1998, **99**, 158–165.
29 W. Temmerman, A. Svane, Z. Szotek, H. Winter and S. Beiden, *Electronic Structure and Physical Properies of Solids*, Springer, 1999, pp. 286–312.

30 R. R. Zope, M. K. Harbola and R. K. Pathak, *Eur. Phys. J. D*, 1999, **7**, 151–155.

31 R. R. Zope, *Phys. Rev. A*, 2000, **62**, 064501.

32 J. Garza, J. A. Nichols and D. A. Dixon, *J. Chem. Phys.*, 2000, **112**, 7880–7890.

33 J. Garza, R. Vargas, J. A. Nichols and D. A. Dixon, *J. Chem. Phys.*, 2001, **114**, 639–651.

34 U. Lundin and O. Eriksson, 2001, **81**, 247–252.

35 S. Patchkovskii, J. Autschbach and T. Ziegler, *J. Chem. Phys.*, 2001, **115**, 26–42.

36 S. Patchkovskii and T. Ziegler, *J. Chem. Phys.*, 2002, **116**, 7806–7813.

37 S. Patchkovskii and T. Ziegler, *J. Phys. Chem. A*, 2002, **106**, 1088–1099.

38 V. Polo, E. Kraka and D. Cremer, *Mol. Phys.*, 2002, **100**, 1771–1790.

39 V. Polo, J. Gräfenstein, E. Kraka and D. Cremer, *Theor. Chem. Acc.*, 2003, **109**, 22–35.

40 T. Tsuneda, M. Kamiya and K. Hirao, *J. Comp. Chem.*, 2003, **24**, 1592–1598.

41 J. Gräfenstein, E. Kraka and D. Cremer, *J. Chem. Phys.*, 2004, **120**, 524–539.

42 J. Gräfenstein, E. Kraka and D. Cremer, *Phys. Chem. Chem. Phys.*, 2004, **6**, 1096–1112.

43 O. A. Vydrov and G. E. Scuseria, *J. Chem. Phys.*, 2004, **121**, 8187.

44 O. A. Vydrov and G. E. Scuseria, *J. Chem. Phys.*, 2005, **122**, 184107.

45 I. Ciofini, C. Adamo and H. Chermette, *J. Chem. Phys.*, 2005, **123**, 121102.

46 M. Lundberg and P. E. M. Siegbahn, 2005, **122**, 224103.

47 O. A. Vydrov, G. E. Scuseria, J. P. Perdew, A. Ruzsinszky and G. I. Csonka, *J. Chem. Phys.*, 2006, **124**, 094108.

48 O. A. Vydrov and G. E. Scuseria, *J. Chem. Phys.*, 2006, **124**, 191101.

49 H. Jónsson, K. Tsemekhman and E. J. Bylaska, Abstracts of Papers of the American Chemical Society, 2007, pp. 120–120.

50 S. Kümmel and L. Kronik, *Rev. Mod. Phys.*, 2008, **80**, 3.

51 J. Messud, P. M. Dinh, P.-G. Reinhard and E. Suraud, 2008, **101**, 096404.

52 J. Messud, P. M. Dinh, P.-G. Reinhard and E. Suraud, 2008, **461**, 316–320.

53 T. Körzdörfer, S. Kümmel and M. Mundt, 2008, **129**, 014110.

54 M. Daene, M. Lueders, A. Ernst, D. Ködderitzsch, W. M. Temmerman, Z. Szotek and W. Hergert, 2009, **21**, 045604.

55 L. Petit, A. Svane, M. Lüders, Z. Szotek, G. Vaitheeswaran, V. Kanchana and W. Temmerman, 2014, **26**, 274213.

56 T. Schmidt, E. Kraisler, L. Kronik and S. Kümmel, 2014, **16**, 14357–14367.

57 M. R. Pederson, T. Baruah, D.-y. Kao and L. Basurto, *J. Chem. Phys.*, 2016, **144**, 164117.

58 S. Lehtola, E. Ö. Jónsson and H. Jónsson, *J. Chem. Theory Comput.*, 2016, **12**, 4296–4302.

59 D.-y. Kao, M. R. Pederson, T. Hahn, T. Baruah, S. Liebing and J. Kortus, *Magnetochemistry*, 2017, **3**, 31.

60 D.-y. Kao, K. Withanage, T. Hahn, J. Batool, J. Kortus and K. Jackson, *J. Chem. Phys.*, 2017, **147**, 164107.

61 K. P. K. Withanage, K. Trepte, J. E. Peralta, T. Baruah, R. Zope and K. A. Jackson, *J. Chem. Theory Comput.*, 2018, **14**, 4122–4128.

62 R. P. Joshi, K. Trepte, K. P. K. Withanage, K. Sharkas, Y. Yamamoto, L. Basurto, R. R. Zope, T. Baruah, K. A. Jackson and J. E. Peralta, *J. Chem. Phys.*, 2018, **149**, 164101.

63 K. Sharkas, L. Li, K. Trepte, K. P. K. Withanage, R. P. Joshi, R. R. Zope, T. Baruah, J. K. Johnson, K. A. Jackson and J. E. Peralta, *J. Phys. Chem. A*, 2018, **122**, 9307–9315.

64 S. Schwalbe, T. Hahn, S. Liebing, K. Trepte and J. Kortus, 2018, **39**, 2463–2471.

65 K. A. Jackson, J. E. Peralta, R. P. Joshi, K. P. Withanage, K. Trepte, K. Sharkas and A. I. Johnson, *J. Phys. Conf. Ser.*, 2019, **1290**, 012002.

66 A. I. Johnson, K. P. Withanage, K. Sharkas, Y. Yamamoto, T. Baruah, R. R. Zope, J. E. Peralta and K. A. Jackson, *J. Chem. Phys.*, 2019, **151**, 174106.

67 K. Trepte, S. Schwalbe, T. Hahn, J. Kortus, D.-Y. Kao, Y. Yamamoto, T. Baruah, R. R. Zope, K. P. K. Withanage, J. E. Peralta and K. A. Jackson, *J. Comput. Chem.*, 2019, **40**, 820–825.

68 S. Schwalbe, L. Fiedler, J. Kraus, J. Kortus, K. Trepte and S. Lehtola, *J. Chem. Phys.*, 2020, **153**, 084104.

69 K. Sharkas, K. Wagle, B. Santra, S. Akter, R. R. Zope, T. Baruah, K. A. Jackson, J. P. Perdew and J. E. Peralta, *Proc. Natl. Acad. Sci.*, 2020, **117**, 11283–11288.

70 J. Vargas, P. Ufondu, T. Baruah, Y. Yamamoto, K. A. Jackson and R. R. Zope, *Phys. Chem. Chem. Phys.*, 2020, **22**, 3789–3799.

71 C. M. Diaz, P. Suryanarayana, Q. Xu, T. Baruah, J. E. Pask and R. R. Zope, *J. Chem. Phys.*, 2021, **154**, 084112.

72 I. Moullet and J. L. Martins, *J.Chem.Phys.*, 1990, **92**, 527–535.

73 T. K. Ghanty and S. K. Ghosh, *J. Phys. Chem.*, 1996, **100**, 17429–17433.

74 B. Champagne, D. H. Mosley, M. Vračko and J.-M. André, *Phys. Rev. A*, 1995, **52**, 178–188.

75 B. Champagne, E. A. Perpète, S. J. A. van Gisbergen, E.-J. Baerends, J. G. Snijders, C. Soubra-Ghaoui, K. A. Robins and B. Kirtman, *J. Chem. Phys.*, 1998, **109**, 10489–10498.

76 S. J. A. van Gisbergen, P. R. T. Schipper, O. V. Gritsenko, E. J. Baerends, J. G. Snijders, B. Champagne and B. Kirtman, *Phys. Rev. Lett.*, 1999, **83**, 694–697.

77 P. Mori-Sánchez, A. J. Cohen and W. Yang, *J. Chem. Phys.*, 2006, **125**, 201102.

78 S. Kuemmel, L. Kronik and J. P. Perdew, *Phys. Rev. Lett.*, 2004, **93**, 213002.

79 H. Sekino, Y. Maeda and M. Kamiya, *Mol. Phys.*, 2005, **103**, 2183–2189.

80 R. Baer and D. Neuhauser, *Phys. Rev. Lett.*, 2005, **94**, 043002.

81 N. T. Maitra and M. Van Faassen, *J. Chem. Phys.*, 2007, **126**, 191106.

82 T. Körzdörfer, M. Mundt and S. Kümmel, 2008, **100**, 133004.

83 D. Pemmaraju, S. Sanvito and K. Burke, *Phys. Rev. B*, 2008, **77**,.

84 A. Ruzsinszky, J. P. Perdew, G. I. Csonka, G. E. Scuseria and O. A. Vydrov, *Phys. Rev. A*, 2008, **77**, 060502.

85 A. Ruzsinszky, J. P. Perdew and G. I. Csonka, *Phys. Rev. A*, 2008, **78**, 022513.

86 J. Messud, Z. Wang, P. M. Dinh, P.-G. Reinhard and E. Suraud, *Chem. Phys. Lett.*, 2009, **479**, 300–305.

87 J. Vargas, M. Springborg and B. Kirtman, *J. Chem. Phys.*, 2014, **140**, 054117.

88 K. P. K. Withanage, S. Akter, C. Shahi, R. P. Joshi, C. Diaz, Y. Yamamoto, R. Zope, T. Baruah, J. P. Perdew, J. E. Peralta and K. A. Jackson, *Phys. Rev. A*, 2019, **100**, 012505.

89 S. Akter, Y. Yamamoto, C. M. Diaz, K. A. Jackson, R. R. Zope and T. Baruah, *J. Chem. Phys.*, 2020, **153**, 164304.

90 C. M. Diaz and Z. R. R. Baruah, Tunna, *Phys. Rev. A*, 2021, **00**, 002800.

91 S. Klüpfel, P. Klüpfel and H. Jónsson, *J. Chem. Phys.*, 2012, **137**, 124102.

92 B. Santra and J. P. Perdew, *J. Chem. Phys.*, 2019, **150**, 174106.

93 R. R. Zope, Y. Yamamoto, C. M. Diaz, T. Baruah, J. E. Peralta, K. A. Jackson, B. Santra and J. P. Perdew, *J. Chem. Phys.*, 2019, **151**, 214108.

94 J. P. Perdew, J. A. Chevary, S. H. Vosko, K. A. Jackson, M. R. Pederson, D. J. Singh and C. Fiolhais, *Phys. Rev. B*, 1992, **46**, 6671–6687.

95 J. P. Perdew, K. Burke and M. Ernzerhof, *Phys. Rev. Lett.*, 1996, **77**, 3865–3868.

96 M. R. Pederson, A. Ruzsinszky and J. P. Perdew, *J. Chem. Phys.*, 2014, **140**, 121103.

97 Z.-h. Yang, M. R. Pederson and J. P. Perdew, *Phys. Rev. A*, 2017, **95**, 052505.

98 M. R. Pederson and C. C. Lin, *J. Chem. Phys.*, 1988, **88**, 1807–1817.

99 J. M. Leonard and W. L. Luken, *Theor. Chem. Acc.*, 1982, **62**, 107–132.

100 W. L. Luken and D. N. Beratan, *Theor. Chem. Acc.*, 1982, **61**, 265–281.

101 W. L. Luken and J. C. Culberson, *Theor. Chem. Acc.*, 1984, **66**, 279–293.

102 P.-O. Löwdin, *Rev. Mod. Phys.*, 1962, **34**, 520–530.

103 M. R. Pederson, *J. Chem. Phys.*, 2015, **142**, 064112.

104 M. R. Pederson and T. Baruah, *Adv. At. Mol. Opt. Phys.*, Academic Press, 2015, vol. 64, pp. 153 – 180.

105 Y. Yamamoto, S. Romero, T. Baruah and R. R. Zope, *J. Chem. Phys.*, 2020, **152**, 174112.

106 R. Van Leeuwen and E. Baerends, *Phys. Rev. A*, 1994, **49**, 2421.

107 M. Grüning, O. V. Gritsenko, S. J. Van Gisbergen and E. Jan Baerends, *J. Chem. Phys.*, 2002, **116**, 9591–9601.

108 A. Banerjee, A. Chakrabarti and T. K. Ghanty, *J. Chem. Phys.*, 2007, **127**, 134103.

109 A. Banerjee, T. K. Ghanty and A. Chakrabarti, *J. Phys. Chem. A*, 2008, **112**, 12303–12311.

110 P. R. Schipper, O. V. Gritsenko, S. J. van Gisbergen and E. J. Baerends, *J. Chem. Phys.*, 2000, **112**, 1344–1352.

111 R. R. Zope, T. Baruah, Y. Yamamoto, C. Basurto, Díaz, L., J. Peralta and K. A. Jackson.

112 K. Jackson and M. R. Pederson, *Phys. Rev. B*, 1990, **42**, 3276–3281.

113 M. Pederson, D. Porezag, J. Kortus and D. Patton, *phys. stat. sol. (b)*, 2000, **217**, 197–218.

114 Y. Yamamoto, L. Basurto, C. M. Diaz, R. R. Zope and T. Baruah.

115 D. Porezag and M. R. Pederson, *Phys. Rev. A*, 1999, **60**, 2840–2847.

116 M. R. Pederson and K. A. Jackson, *Phys. Rev. B*, 1990, **41**, 7453–7461.

117 A. Brakestad, S. R. Jensen, P. Wind, M. D'Alessandro, L. Genovese, K. H. Hopmann and L. Frediani, *J. Chem. Theory Comput.*, 2020, **16**, 4874–4882.

118 M. J. Frisch, G. W. Trucks, H. B. Schlegel, G. E. Scuseria, M. A. Robb, J. R. Cheeseman, G. Scalmani, V. Barone, G. A. Petersson, H. Nakatsuji, X. Li, M. Caricato, A. V. Marenich, J. Bloino, B. G. Janesko, R. Gomperts, B. Mennucci, H. P. Hratchian, J. V. Ortiz, A. F. Izmaylov, J. L. Sonnenberg, D. Williams-Young, F. Ding, F. Lipparini, F. Egidi, J. Goings, B. Peng, A. Petrone, T. Henderson, D. Ranasinghe, V. G. Zakrzewski, J. Gao, N. Rega, G. Zheng, W. Liang, M. Hada, M. Ehara, K. Toyota, R. Fukuda, J. Hasegawa, M. Ishida, T. Nakajima, Y. Honda, O. Kitao, H. Nakai, T. Vreven, K. Throssell, J. A. Montgomery, Jr., J. E. Peralta, F. Ogliaro, M. J. Bearpark, J. J. Heyd, E. N. Brothers, K. N. Kudin, V. N. Staroverov, T. A. Keith, R. Kobayashi, J. Normand, K. Raghavachari, A. P. Rendell, J. C. Burant, S. S. Iyengar, J. Tomasi, M. Cossi, J. M. Millam, M. Klene, C. Adamo, R. Cammi, J. W. Ochterski, R. L. Martin, K. Morokuma, O. Farkas, J. B. Foresman and D. J. Fox, *Gaussian 16 Revision B.01*, 2016, Gaussian Inc. Wallingford CT.

119 P. Bhattarai, K. Wagle, C. Shahi, Y. Yamamoto, S. Romero, B. Santra, R. R. Zope, J. E. Peralta, K. A. Jackson and J. P. Perdew, *J. Chem. Phys.*, 2020, **152**, 214109.

120 J. Sun, A. Ruzsinszky and J. P. Perdew, *Phys. Rev. Lett.*, 2015, **115**, 036402.

121 S. Romero, Y. Yamamoto, T. Baruah and R. R. Zope, *Phys. Chem. Chem. Phys.*, 2021, **23**, 2406–2418.

122 K. P. K. Withanage, P. Bhattarai, J. E. Peralta, R. R. Zope, T. Baruah, J. P. Perdew and K. A. Jackson, *J. Chem. Phys.*, 2021, **154**, 024102.

123 P. Bhattarai, B. Santra, K. Wagle, Y. Yamamoto, R. R. Zope, K. A. Jackson and J. P. Perdew, *J. Chem. Phys.*, 2021, **154**, 094105.